ORIENTED FILTERS FOR VESSEL CONTRAST ENHANCEMENT WITH LOCAL DIRECTIONAL EVIDENCE

Suvadip Mukherjee and Scott T. Acton

Department of Electrical and Computer Engineering, University of Virginia, Charlottesville, VA

ABSTRACT

Vascular structures occur in abundance within biomedical and biological image processing applications. From detecting retinal blood vessels to analyzing shape and connectivity of neurons, segmentation of vascular structures has received significant attention in the literature. Robust segmentation often demands a preprocessing stage involving enhancement of the tubular objects. We propose a novel method to enhance vascular structures from low contrast images by incorporating evidence of neighboring tubular structures in addition to the local vessel detection. We show that the proposed algorithm, called local directional evidence (LDE), is capable of handling bifurcations, intensity inhomogeneity and complex geometry of the vessels, thus providing a robust preprocessing for segmentation. Experiments on a collection of biological images containing vascular objects suggest efficacy of LDE when used as a precursor to segmentation. We observe that LDE improves the average segmentation performance by 63% on our database over the vessel enhancing filter of [1].

1. INTRODUCTION

Segmenting vascular structures is a salient problem in the biomedical imaging literature. Sample applications include, but are not limited to, segmenting arteries and veins from magnetic resonance angiography (MRA) images of different organs such as brain, liver, retina etc. and identifying neuron morphology from confocal microscopy. Often the raw images suffer from low contrast and clutter, which makes segmentation a challenging prospect. As a result a preprocessing step is generally introduced to enhance the vascular structures prior to segmentation. Naturally, efficacy of these segmentation techniques depends heavily on the preprocessing quality. Hence, it is desired that the vessel enhancement algorithm be capable of identifying the correct structure while attenuating false positives.

Frangi *et al*. [1] proposed a multiscale algorithm for identifying vascular structures by studying the eigenvalues of the hessian matrix of an image. This vessel enhancement filter is widely used for its simplicity and intuitive geometric understanding. However, this popular vessel enhancing algorithm suffers from some deficiencies. First, intensity variation across the vessels compromises the enhancement result.

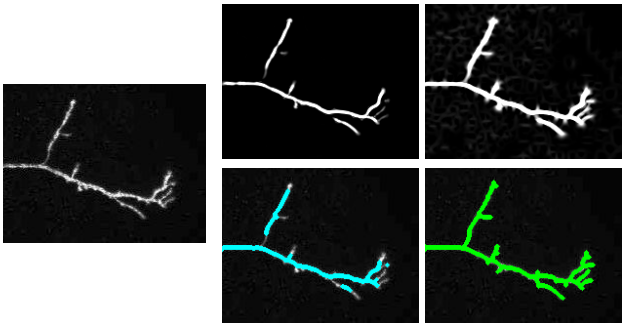

Fig. 1: A noisy confocal microscopy image of a dendrite is shown in the first column. The results of vessel enhancement due to Frangi's filter [1] and LDE is shown in the top row, left to right. The bottom row displays the segmented centerline using [1] in cyan and LDE in green.

This is primarily because the algorithm is inherently local and does not utilize neighboring vessel evidence. Furthermore, the method of [1] assumes that the vessel filaments can be approximated as an ellipsoid, an assumption which is violated at bifurcation and vessel bends (see Fig. 1). As a result, the output of this vesselness filter sometimes requires an additional postprocessing such as vessel diffusion [2], tensor voting [3] etc.

Krissian *et al*. [4] suggests a model based approach where the vessels are modeled as cylinders with circular and elliptical cross-section. Again, vessel detection is performed via eigenvalue analysis of these models. Matched filter based techniques have been proposed [5] for retinal blood vessel extraction. Other notable work in this regard includes mathematical morphology based technique of Wilkinson and Westenberg [6] and the line filter by Sato *et al*. [7]. A comprehensive survey of recent vessel detection and enhancement techniques is presented in [8].

1.1. Vessel detection with oriented filters

Vessel detection problem can be posed as finding the maximum response when the image is convolved with a suitable template (see Fig. 2(b-c)) at multiple orientations. Freeman and Adelson [9] introduced a class of filters, namely steerable filters, which can be rotated by taking a linear combination of a few basis filters. For ridge detection, steerable filters based on second order derivatives of the gaussian function are popular due to computational simplicity. Jacob and

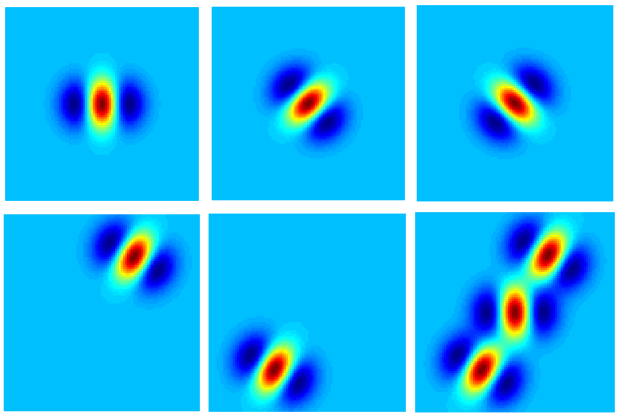

Fig. 2: The top row shows oriented vessel detector kernels r_d for $\theta = 0, -\frac{\pi}{4}, \frac{\pi}{4}$ from left to right. The bottom row shows from left to right: forward evidence kernel r_f, backward evidence kernel r_b and the superimposed LDE kernels for $\theta = 0$ and $\psi_1 = \psi_2 = \frac{\pi}{6}$. We choose the offset to an exaggerated value $d = 4\sigma$ for better visual clarity.

Unser [10] showed that efficient ridge templates can be computed using directional gaussian second derivatives. The hessian $H_\sigma(p)$ of a 2-d image $f(p)$, convolved with a gaussian kernel $g(p;\sigma) = \frac{1}{\sqrt{2\pi}\sigma} e^{-\frac{x^2+y^2}{2\sigma^2}}$ at a position $p = (x, y)$ is given by

$$H_\sigma(p) = \begin{pmatrix} g_{xx}(p) & g_{xy}(p) \\ g_{xy}(p) & g_{yy}(p) \end{pmatrix} * f(p) \tag{1}$$

The second derivative of the smoothed image in a direction $\mathbf{u}_\theta = (\cos\theta, \sin\theta)^T$ is obtained as $\mathcal{R}_d(p,\theta;\sigma) = \mathbf{u}_\theta^T H_\sigma(x,y)\mathbf{u}_\theta$. Simplifying this, we obtain the directional vessel response as follows:

$$\mathcal{R}_d(p,\theta;\sigma) = r_d(p,\theta;\sigma) * f(p) \tag{2}$$

$$r_d(p;\theta,\sigma) = g_{xx}\cos^2\theta + g_{yy}\sin^2\theta + g_{xy}\sin 2\theta \tag{3}$$

The vesselness score at scale σ is computed as

$$\mathcal{R}^*_d(p;\sigma) = \max_\theta \mathcal{R}_d(p,\theta;\sigma) \tag{4}$$

Here $r_d(p;\sigma,\theta)$ denotes a local vessel detector template, parameterized by the angle θ. A higher value of the inner product of the shifted and rotated version of the template $r_d(p,\theta;\sigma)$ at each image pixel provides evidence for presence of a vascular object orientated at an angle $\pi/2 + \theta$ and scale σ. A set of three detector kernels are shown in Fig. 2, top row. Despite the property of steerability of the local detection template r_d, such detectors are prone to local intensity variation across the vascular structures. Moreover, the designed steerable kernel in (3) is suited for detecting homogeneous vessels and is incapable of handling complicated structures such as vessel bifurcations. The idea proposed by Jacob and Unser [10] aims at refining the ridge response using non-maximal suppression and improving the SNR. While this reduces the false positives significantly, the method is not particularly suited at handling bifurcations and complicated vessel morphology. Qian et al. [11] propose a solution by investigating the local neighborhood of a point to find evidence of vascular structure. However, the authors make a strong assumption that the vessel intensities remain constant over the neighborhood, which is often violated due to inhomogeneities arising from imaging artifacts.

The motivation for this work comes from the fact that the widely used vessel enhancing filters [1, 4, 6, 7] are less adept at detecting vascular regions of low intensity and bifurcation points. Our proposed method, called Local Directional Evidence (LDE) uses a set of oriented filters to determine local evidence of vessels. This set of oriented filters, in addition to the local detector filter shown in (4) is used to enhance low contrast vascular structures with complicated morphology.

2. VESSEL ENHANCEMENT WITH LOCAL DIRECTIONAL EVIDENCE (LDE)

As mentioned before, a major defect with current vessel enhancement methods is the inability to tackle local intensity variations and complex morphology. This creates further artifacts during segmentation, where multiple fragments are created which again require further connectivity analysis [12, 13]. We hypothesize that one possible way to handle this problem is to boost the local detector response (3) with evidence of a vessel in a given local neighborhood. However, unlike the method proposed in [11], we search for oriented vessels in the neighboring region, thus never relying on the homogeneity of the structures.

The local directional evidence is provided by convolving the image with another set of oriented filters– forward filters $r_f(p;\sigma,\psi_1)$ and backward filters $r_b(p;\sigma,\psi_2)$. We compute the set of local evidence filters in the following manner:

$$r_f(p;\sigma,\psi_1) = r_d(x + d\cos(\theta+\psi_1), y + d\sin(\theta+\psi_1)) \tag{5}$$

$$r_b(p;\sigma,\psi_2) = r_d(x - d\cos(\theta+\psi_2), y - d\sin(\theta+\psi_2)) \tag{6}$$

Here $\theta - \alpha \le \psi_1, \psi_2 \le \theta + \alpha$ is a set of orientations used to detect evidence of vessels in a local angular region near the detection point. The offset parameter $d > 0$ controls the locality of the evidence filters. While a low value of d does not contribute enough, a significantly larger value may introduce false positives by predicting vessels which do not belong to the same structure. For experimental evaluation, we choose $\alpha = \frac{\pi}{3}$ since abrupt bending in vessels is rare in our applications which includes neurons and retinal blood vessels. The value of $d \le \sqrt{2}\sigma$ has been observed to give good balance between localization and accuracy of the evidence filters. A set of evidence kernels is shown in the second row of Fig. 2 with $\theta = 0$ and $\psi_1 = \psi_2 = \frac{\pi}{6}$.

The response due to the evidence kernels are given by $\mathcal{R}_f(p;\sigma,\psi_1) = r_f(p;\sigma,\psi_1) * f(p)$ and $\mathcal{R}_b(p;\sigma,\psi_2) =$

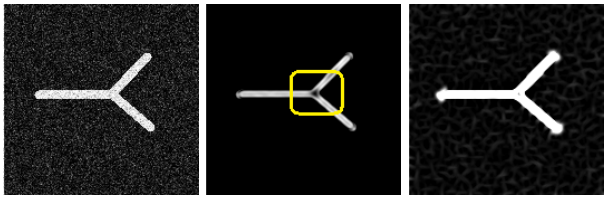

(a) (b) (c)

Fig. 3: A simulated image of a Y-junction is shown in (a). The enhancement result using [1] is shown in (b) and the response at the junction highlighted by the yellow rectangle. (c) The LDE response.

$r_b(p;\sigma,\psi_2) * f(p)$. The overall vessel enhancement response is calculated in the following manner:

$$\mathcal{R}^*(p;\sigma) = \max_{\theta} \mathcal{R}_d(p) + \mathcal{R}_b^*(p) + \mathcal{R}_f^*(p) \tag{7}$$
$$\mathcal{R}_b^*(p) = \max_{\psi_1} \mathcal{R}_b(p) \text{ and } \mathcal{R}_f^*(p) = \max_{\psi_2} \mathcal{R}_f(p)$$

The dependence on the variables θ, ψ_1, ψ_2 is implied. To incorporate vessels with varying thickness in our solution, a multiscale approach is desirable. Over a range of scales $\mathcal{S} = \{\sigma_{min}, \ldots, \sigma_{max}\}$ scale space vesselness response is calculated as follows:

$$\mathcal{V}(p) = \max_{\sigma \in \mathcal{S}} \mathcal{R}^*(p;\sigma) \tag{8}$$

The range of scales is problem specific and is determined from prior biological knowledge about the thickness of the vascular structures.

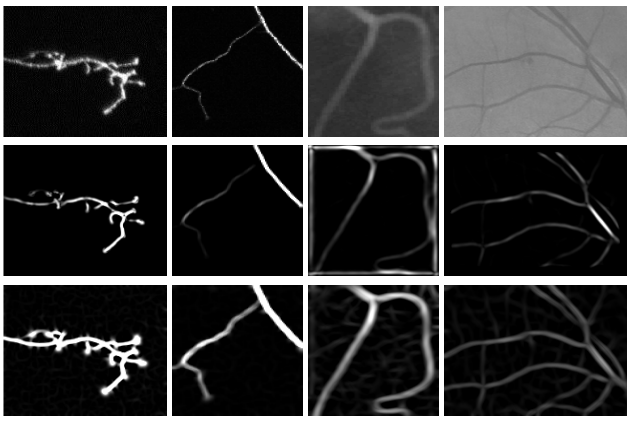

(a) (b) (c) (d)

Fig. 4: First row: (a-b) Confocal microscopy neuron images of the *Drosophila* larva. (c-d) Retinal blood vessels. The second row shows the enhancement results using [1]. Vessel enhancement due to LDE is shown in the bottom row.

2.1. Discussion of LDE

The most significant contribution of this paper is in the design of the directional vessel evidence templates. Unlike the standard ridge detector template shown in the first row of Fig. 2, the forward and backward evidence templates in (6), together with the detector template (3), provide an effective way to approximate the vessels as flexible oriented structures, as opposed to the local rigid structure which results from using the detector template only. A set of vessel templates are shown in Fig. 2, second row for illustration. The advantage of using the oriented evidence filters is that complex vessel geometry such as sharp bends and bifurcations can also be handled. While the traditional eigenvalue based method proposed by Frangi [1] rejects branch points as candidate vessel point (see Fig. 3(b)), LDE is able to tackle the bifurcation by virtue of the local evidence filters (see Fig. 3(c)). As we would show in the next section, LDE improves segmentation results significantly when used as a preprocessing tool.

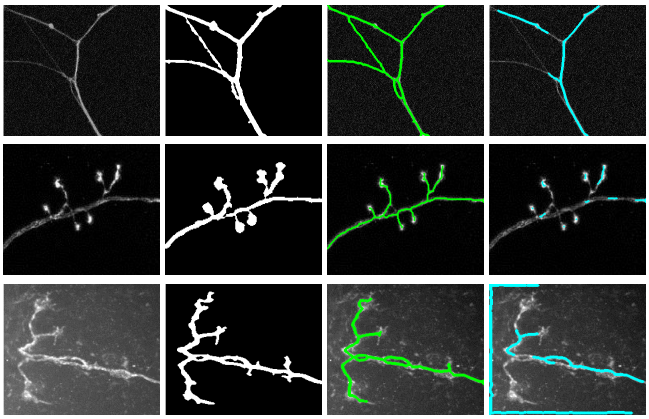

(a) (b) (c) (d)

Fig. 5: Neuron segmentation results. (a) 2-d projection of confocal microscopy stack. (b) Binary segmentation after LDE based enhancement. (c) Traced centerline for LDE based segmentation and (d) Centerline tracing using [1]+segmentation.

3. EXPERIMENTAL RESULTS

To demonstrate the efficacy of our method, we perform analysis on a set of fifteen images of containing vascular objects, obtained from different modalities. Our dataset consists of 2-d mean intensity projection of neuron images of the fruit fly *Drosophila* and retinal blood vessels from the online database [14]. Enhancement results on a subset of images are shown in Fig. 4. The first row shows 2-d images of neurons and retinal blood vessels, and the enhancement results using [1] and LDE are displayed in the second and third rows respectively. Qualitative enhancement results suggest LDE is better equipped at detecting junctions and sharp turns of the vessels as well as inhomogeneous intensity, compared to the hessian based method [1], where the locality of the approach creates a non-homogeneous vesselness response.

Another way of identifying the performance benefit of using LDE is by evaluationg the segmentation results of the vessel enhanced image. Fig. 5(a) depicts three neuron images of the fruit fly *Drosophila*. The segmentation of the preprocessed images is performed using Otsu's pixel classification scheme [15]. The binarized output corresponding to

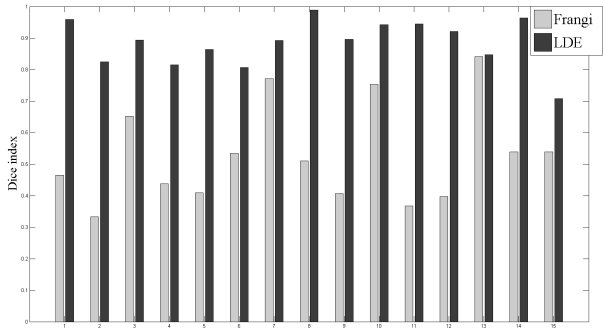

Fig. 6: The dice index for each image is shown for the segmentation results for each image in the dataset. Segmentation is performed as a post processing step for both and LDE and the method in [1].

LDE based preprocesssing is shown in Fig. 5(b) and the obtained centerline is plotted in (c). Corresponding neuron centerlines due to images preprocessed using [1] are plotted in Fig. 5(d). It is seen in Fig. 5(d) that the final neuron tracing is affected by the non uniform response of [1], which requires further connectivity analysis to get the desired neuron segmentation [12, 13].

Segmentation performance is quantitatively evaluated using the Dice index. The Dice index $\mathcal{D} \in [0, 1]$ for segmentations A and B is given by $\mathcal{D}(A, B) = 2|A \cap B|/|A| + |B|$. If A denotes ground truth segmentation, and B is the experimentally obtained result, a Dice value closer to 1 indicates superior performance. Since the segmentation performance is directly correlated to enhancement efficiency, an improved segmentation result suggests efficient preprocessing. Dice indices for different images are plotted in Fig. 6. The images are preprocessed with both Frangi's method and LDE, and the dice values corresponding to Otsu's segmentation is plotted for both the algorithms. It is observed from the quantitative results that preprocessing with LDE has superior performance over [1], producing an average Dice index of 0.88 as compared to 0.57 using the latter.

4. CONCLUSION

A novel technique for enhancing tubular structures is proposed. A set of oriented evidence filters are used to boost the vessel detection process. Qualitative and quantitative performance suggest superiority of LDE over the popular hessian based method due to [1], with a performance improvement of over 60% on the set of images. The developed vessel enhancement technique is being incorporated in our automated neuron tracing software [12, 13], which is being used to map the *Drosophila* neurome.

5. REFERENCES

[1] A. F. Frangi *et al.*, "Multiscale vessel enhancement filtering," in *MICCAI*, pp. 130–137. Springer, 1998.

[2] R. Manniesing *et al.*, "Vessel enhancing diffusion: A scale space representation of vessel structures," *Medical Image Analysis*, vol. 10, no. 6, pp. 815–825, 2006.

[3] A. Narayanaswamy *et al.*, "3-d image pre-processing algorithms for improved automated tracing of neuronal arbors," *Neuroinformatics*, vol. 9, no. 2-3, pp. 219–231, 2011.

[4] K. Krissian *et al.*, "Model-based detection of tubular structures in 3d images," *Computer Vision and Image Understanding*, vol. 80, no. 2, pp. 130–171, 2000.

[5] M. Sofka and C. V. Stewart, "Retinal vessel centerline extraction using multiscale matched filters, confidence and edge measures," *IEEE Trans. Med. Imag.*, vol. 25, no. 12, pp. 1531–1546, 2006.

[6] M. Wilkinson and M. Westenberg, "Shape preserving filament enhancement filtering," in *MICCAI*. Springer, 2001, pp. 770–777.

[7] Y. Sato *et al.*, "Three-dimensional multi-scale line filter for segmentation and visualization of curvilinear structures in medical images," *Medical Image Analysis*, vol. 2, no. 2, pp. 143–168, 1998.

[8] D. Lesage *et al.*, "A review of 3d vessel lumen segmentation techniques: Models, features and extraction schemes," *Medical Image Analysis*, vol. 13, no. 6, pp. 819–845, 2009.

[9] W. T. Freeman and E. H Adelson, "The design and use of steerable filters," *IEEE Trans. Pattern Anal. Machine Intell.*, vol. 13, no. 9, pp. 891–906, 1991.

[10] M. Jacob and M. Unser, "Design of steerable filters for feature detection using canny-like criteria," *IEEE Trans. Pattern Anal. Machine Intell.*, vol. 26, no. 8, pp. 1007–1019, 2004.

[11] X. Qian *et al.*, "A non-parametric vessel detection method for complex vascular structures," *Medical Image Analysis*, vol. 13, no. 1, pp. 49–61, 2009.

[12] S. Mukherjee *et al.*, "Tree2tree2: Neuron tracing in 3d," in *IEEE Intl. Symp. on Biomedical Imaging*, 2012, pp. 448–451.

[13] S. Basu *et al.*, "Segmentation and tracing of single neurons from 3d confocal microscope images," *IEEE J. Biomedical and Health Informatics*, vol. 17, no. 2, pp. 319–335, 2013.

[14] J. Staal *et al.*, "Ridge-based vessel segmentation in color images of the retina," *IEEE Trans. Med. Imag.*, vol. 23, no. 4, pp. 501–509, 2004.

[15] N. Otsu, "A threshold selection method from gray-level histograms," *Automatica*, vol. 11, no. 285-296, pp. 23–27, 1975.